Chapter 4

AGC3 kinase-calmodulin signaling in phyllotaxis

Yuanwei Fan, Jasmijn van der Weide, Remko Offringa

Molecular and Developmental Genetics, Institute Biology Leiden, Leiden University, Sylviusweg 72, 2333 BE Leiden, the Netherlands

Summary

Phyllotaxis, or the arrangement of lateral organs on a plant stem, is determined by the pattern of organ primordium initiation in the shoot apical-, inflorescence- or flower meristem. The position of primordium initiation is in part instructed by the unequal distribution of auxin in the meristem epidermis, which is driven by the asymmetric subcellular localisation of the auxin efflux carrier PIN1. The localization of PIN1 is dependent on phosphorylation of three specific serine residues in its central hydrophilic loop by the AGC3 protein kinases PID, WAG1 and WAG2. Here we show that PIN1 phosphorylation by the three AGC3 kinases is important for maintaining the normal spiral phyllotaxis (137.5 º angle) in *Arabidopsis*, and that deregulation of PIN1 phosphorylation dynamics leads to irregular phyllotaxis, varying from absence of primordium initiation to a switch from the normal spiral (137.5 ° angle) to a decussate-like (alternating 180 ° and 90 ° angles) pattern. In addition, auxin, mechanical stress and overexpression of the calmodulin-like protein CML12/TCH3 trigger Ca^{2+}-dependent internalization of PID in the inflorescence meristem. The enhanced variation in the divergence angle between flowers in *TCH3* overexpression or *tch3* loss-of-function mutant inflorescences suggests that a dynamic recruitment of the kinase by TCH3 is required for a regular spiral phyllotaxis. Our results suggest the involvement of the AGC3 kinase-CML signalling complex in modulating of the phyllotactic pattern in response to auxin and mechanical stress.

Introduction

A remarkable feature of plant development is the regular arrangement of lateral organs (leaves and flowers) around a plant stem, which is called phyllotaxis. In the developing shoot, existing primordia arising from the shoot apical meristem (SAM) and the inflorescence meristems (IMs) are involved in determining the position where new primordia will be formed (Reinhardt et al., 2005). Auxin produced by the existing primordia is redistributed by polar cell-to-cell transport, which generates a new maximum that serves as initiation point for a new primordium (Reinhardt et al., 2003; Tanaka et al., 2006). This polar auxin transport is mediated by PIN-FORMED (PIN) and AUX1/LAX1 proteins, which function as auxin efflux- and influx carriers, respectively (Tanaka et al., 2006). The direction of auxin transport is determined by the asymmetric subcellular localization of the PIN auxin efflux carriers, which is dependent on phosphorylation of the large central hydrophilic loop by PINOID (PID) and the redundantly functioning WAG1 and WAG2 protein kinases (Friml et al., 2004; Dhonukshe et al., 2010; Huang et al., 2010).

PIN1, the founding member of the PIN protein family, plays an essential role in regulating phyllotaxis. The dynamic subcellular localization of PIN1 in the epidermis of the SAM follows a specific pattern, leading to the transport of auxin towards the sites of organ formation (Reinhardt et al., 2003; Heisler et al., 2005). Proper phosphorylation of PIN1 is essential for the regulation of its subcellular localization and the formation of organs in the IM. In *pin1* mutant IMs expressing non-phosphorylatable PIN1:GFP, with the serine phosphorylation targets substituted for alanines, the mutant PIN1 is localized at the basal instead of the apical membrane of epidermis cells and the meristem is defective in lateral organ formation (Huang et al., 2010). Based on the apparent role of auxin and PIN1 in the formation of organs at the SAM, Reinhardt and coworkers proposed that as a consequence of auxin transport to the primordia, the concentration of auxin in tissues surrounding the primordia will be low and thus, no organs will be formed there; only at a certain distance from existing primordia, new auxin maxima can arise, leading to new primordia (Reinhardt et al., 2003). Using mathematical modelling, it was shown that these simple assumptions can generate patterns similar to the phyllotactic patterns occurring in nature (Jonsson et al., 2006; Smith et al., 2006).

Although models based only on biochemical processes can explain phyllotactic patterns, several lines of evidence suggest that cells in the meristem that constantly produces new organs experience mechanical stress, and that mechanical stress might also be directing phyllotactic patterns (Besnard et al., 2011; Mirabet et al., 2011). Mathematical models

indicate that mechanical and biochemical mechanisms can reinforce each other (Newell et al., 2008). A link between mechanical forces and plant development has been described by Hamant and co-workers (Hamant et al., 2008). Microtubules are well known to determine the direction of cell growth. In cells of the SAM the orientation of microtubules is altered in response to changes in stress patterns or to externally applied mechanical constraints (Hamant et al., 2008). Recently, it has been shown that the polar localization of PIN1 proteins also responds to changes in mechanical stress patterns and that PIN1 localization and microtubule orientation are highly correlated in the SAM. A likely role for PID in mechanical stress signalling was suggested based on the absence of PIN1 re-polarization following mechanical stress in *pid* loss-of-function mutants (Heisler et al., 2010). The question now arises how PIN1 orientation is regulated by mechanical stress. Since the subcellular localization of PIN1 depends on phosphorylation by PID, molecules that regulate PID function can be involved in regulating PIN1 orientation in response to mechanical stress.

One of the first responses in cells that are under mechanical stress is a rapid increase in the cytosolic Ca^{2+} levels (Monshausen et al., 2009). Based on the results in Chapters 2 and 3, elevated Ca^{2+} levels can be translated into changes in PIN localisation by calmodulin-mediated sequestration of PID and WAG2 from the plasma membrane to the cytosol. The AGC3 kinase-calmodulin signalling complex is therefore a strong candidate to couple mechanical stress to PIN1 orientation during phyllotaxis.

The first calmodulin-like protein identified as PID binding protein was TOUCH3 (Benjamins et al., 2003). The *TCH3* gene was originally identified as a gene whose transcription is induced by several stimuli, including rain, touch and wind (Braam and Davis, 1990). *TCH3* expression can be induced by auxin (Antosiewicz et al., 1995) and increased Ca^{2+} concentrations (Braam, 1992). Since TCH3 seems to regulate PID activity in a Ca^{2+}-dependent manner (Benjamins et al., 2003)(Chapters 2 and 3), and mechanical stimuli can result in increased cytoplasmic Ca^{2+} levels (Trewavas and Knight, 1994; Haley et al., 1995), TCH3 is the perfect candidate to couple mechanical signals to reorientation of PIN polarity. In this chapter, we studied the possible involvement of the AGC3 kinases in phyllotaxis, and we also tested the possibility that *TCH3* is involved in regulating phyllotaxis. Our results show that the AGC3 kinases PID, WAG1 and WAG2 are involved in maintaining the normal spiral phyllotaxis (137.5 ºangle) in *Arabidopsis*, and that deregulation of PIN1 phosphorylation dynamics leads to irregularities, and frequently results in switches from spiral to decussate (alternating 180 ºand 90 ºangles) phyllotaxis. *tch3-3* loss-of-function mutants showed a

distichous phyllotaxis pattern and changes in its activity led to enhanced variation in the divergence angle between primordia in the IM. Our results suggest the involvement of the AGC3 kinase-TCH3 signalling complex in controlling the phyllotactic pattern, in response to auxin and mechanical stress dynamics in the *Arabidopsis* SAM and IM.

Results

AGC3 kinases play a role in phyllotaxis

To investigate the role of PID and its close homologs WAG1 and WAG2 in phyllotactic patterning, the divergence angles between subsequent lateral organs of rosette leaves were measured in wild-type *Arabidopsis* (Col-0), the *pid-14*, *wag1 wag2*, *pid wag1*, *pid wag2* and *pid wag1 wag2* loss-of-function mutants and in *35S::PID* overexpression plants. In addition, we performed measurements on *pin1* mutant plants expressing the complementing *PIN1::PIN1-GFP* fusion gene, or the *PIN1::PIN1-GFP S123A* loss-of-phosphorylation or *PIN1::PIN1-GFP S123E* phosphomimic version (Table 1).

Table 1. AGC3 kinases reduce the variation in divergence angle in *Arabidopsis* rosette leaf phyllotaxis

Plant line	Mean	SD	p1	#plants	#angles	Angle>180 °	p2
Col-0	138.0	13.3		8	66	0	-
Col-0 (II)	138.8	17.1		11	75	0	-
pid (II)	137.2	17.5	0.88	9	81	1	0.97
wag1 wag2	139.0	19.3	0.001	12	111	1	0.79
pid wag1	125.4	33.6	$< 10^{-3}$	3	29	1	0.67
pid wag2	148.8	40.3	$< 10^{-3}$	5	41	3	0.10
pid wag2 (II)	154.3	50.2	$< 10^{-3}$	8	50	9	0,005
pid wag1	137.7	26.8	$< 10^{-3}$	7	51	1	0.90
35S::PID	140.0	25.1	$< 10^{-3}$	10	83	1	0.91
PIN1-GFP	136.3	17.6	0.82	11	76	0	1
PIN1-GFP	146.0	42.2	$< 10^{-3}$	13	64	6	0.02
PIN1-GFP	135.7	21.2	$< 10^{-3}$	12	84	0	1
tch3-3	138.4	16.6	0.052	12	112	1	0.79
35S::TCH3-2	137.1	17.3	0.025	11	88	0	1

Per plant line the mean divergence angle and the standard deviation are given. (II) indicates plant lines that were tested in a second experiment. Number of plants and the total number of angles on which the mean values are based are provided. Also the number of divergence angles that are larger than 180 degrees is indicated. p1 indicates the significance level given by an F test of equality of the variance of divergence angles in a specific line compared to wild-type (Col-0). p2 indicates the probability value for the Pearson's Chi squared test ($P < 0.05$ for significant difference with Col-0) for the fraction of angles that is larger than 180 degrees as compared to that in wild-type plants.

We focused our analysis on rosettes, as the inflorescence phyllotaxis is too much disturbed in those mutants that form pin-like structures. The mean divergence angle in Col-0 rosettes approximated the 'golden angle' of 137.5 ° for spiral phyllotaxis (Mitchison, 1977; Kuhlemeier, 2007) (Table 1). However, the variation in values as indicated by standard deviation was quite high (Table 1). The rosette phyllotaxis of the *pid* mutant was comparable to that of wild type, but all double and triple mutant combinations of *pid*, *wag1* and *wag2* showed a significantly increased variation in the divergence angles, which is in line with the functional redundancy between these kinases. The fact that the variation in the *pid wag1 wag2* triple mutant plants was significantly higher compared to the *wag1 wag2* double mutants ($p = 0.0047$), confirmed the relative importance of *PID* for the maintenance of the spiral phyllotactic pattern.

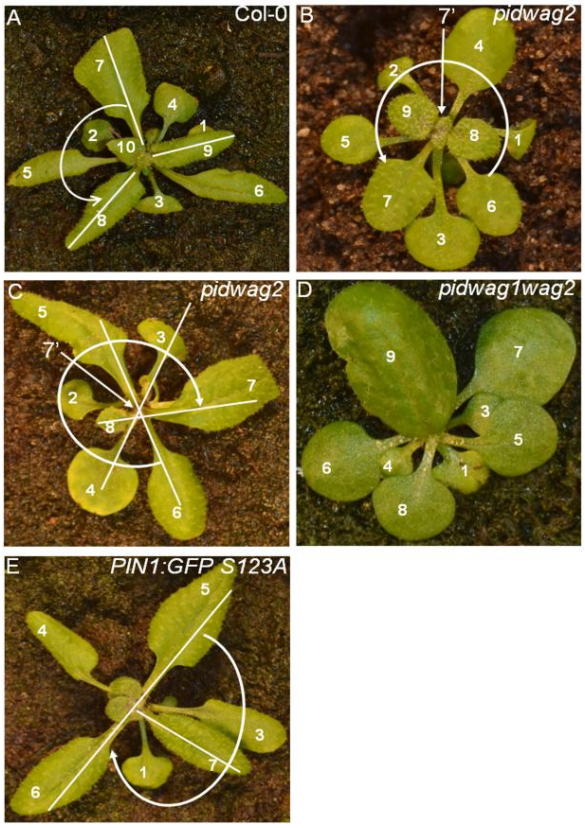

Figure 1. The phenotypes of AGC3 kinase mutants

(A) Normal phyllotaxis in a rosette of wild-type *Arabidopsis* (Col-0), with divergence angles approaching the 'golden angle' of 137.5°. (B-E) irregular phyllotaxis in *pid wag2*, *pid wag1 wag2* and *pin1 PIN1::PIN1:GFP S123A* mutant rosettes. The divergence angles in *pid wag2* mutant rosettes (B, C) vary significantly compared to wild-type rosettes. An angle of 270 ° observed in some rosettes suggests failure of primordium initiation (white straight arrow in B and C), whereas the rosette in (C) also has a decussate appearance (subsequent angles of 180 ° and 90 °). *pid wag1 wag2* rosettes have a dwarf appearance with a relatively normal spiral phyllotaxis, except for the 270 ° angle between leaves 4 and 5 (D). *pin1 PIN1::PIN1:GFP S123A* plants occasionally show a decussate phyllotaxis. The white curved arrow indicates the turn of the phyllotaxis.

Unexpectedly, the standard deviation in *pid wag1 wag2* triple mutants was lower than in *pid wag2* double mutants (p=0.0067), suggesting that the *wag1* mutation somehow counteracts the effect of *wag2*. The mean value for the divergence angle of the *pid wag1* double mutant was lower than that of wild type, whereas it was higher for the *pid wag2* mutant combination. This together with the fact that the value of *pid wag1 wag2* is closer to the angle in wild-type (Col-0) *Arabidopsis*, suggests that *WAG1* and *WAG2* antagonistically contribute to maintaining the 137.5 ° divergence angle. However, the strong dwarf phenotype of the *pid wag1 wag2* triple mutant rosette compared to all other mutants (Figure 1D) corroborates the previously shown redundant activity of the three kinase genes (Dhonukshe et al., 2010).

The involvement of the three AGC3 kinases in phyllotaxis was confirmed by the results of the *PIN1::PIN1:GFP S123A* loss-of-phosphorylation or *PIN1::PIN1:GFP S123E* phosphomimic lines. In both cases a significant increase in the variation in the divergence angle was observed, with loss-of-phosphorylation having a more severe effect, indicating that for proper phyllotaxis the PIN1 phosphorylation dynamics is important.

For those mutant lines that did not form pin-like inflorescences we also determined the divergence angles between subsequent flower petioles on inflorescence stems. All mutant lines tested (*35S:PID*, *wag1 wag2* and *PIN1-GFP S123E*) showed a significantly higher standard deviation in the divergence angle compared to wild-type (Table 2). These results confirm the involvement of AGC3 kinase-mediated PIN1 phosphorylation in the stability of the phyllotactic pattern.

Table 2. AGC3 kinases reduce the variation in the divergence angle in inflorescence phyllotaxis

Plant line	Mean	SD	P1	#Angles	angles > 180 °	P2
Col-0	142.1	26.8	-	74	2	-
Col-0 (II)	139.6	19.7	-	123	9	-
tch3-3	138.1	44.0	$< 10^{-3}$	151	13	0.17
35S::TCH3	142.9	35.8	0.006	163	11	0.34
35S::PID	133.5	53.5	$< 10^{-3}$	111	8	0.32
wag1 wag2	129.8	37.7	0.002	118	5	0.88
PIN1-GFP (II)	139.8	19.3	0.82	123	7	0.80
PIN1-GFP S123E	128.7	51.9	$< 10^{-3}$	106	11	0.10

Mean divergence angle and standard deviation (SD) of divergence angles between subsequent rosette leaves and pedicels in Col-0 and mutant inflorescences. P1 indicates the significance level given by an F test of equality of the variance of divergence angles in a specific line compared to wild-type. P2 indicates the probability value for the Pearson's Chi squared test ($P < 0.05$ for significant difference with Col-0) for the fraction of angles that is larger than 180 ° as compared to the fraction in wild-type plants.

AGC3 kinase-mediated PIN1 phosphorylation is required for spiral phyllotaxis

For wild-type *Arabidopsis*, the divergence angle between rosette leaves was approximately 137.5 ° and, as reported before, the phyllotactic spiral was either clockwise or anticlockwise (Figure 1A;(Landrein et al., 2013)). Divergence angles of more than 180 ° were occasionally observed in *pid*, *pid wag1*, *pid wag1 wag2*, *wag1 wag2* and *35S::PID* rosettes, and significantly more frequent in *pin1 PIN1::PIN1:GFP S123A* and *pid wag2* mutant rosettes (Table 1). When we carefully studied *pid wag2* rosettes containing these larger divergence angles, in several cases such angles appeared to be two times the normal angle (275 °), and to be followed by a normal wild-type angle (Figure 1B). Such a large angle can be explained by the failure of primordium initiation at one position, followed by a successful initiation event at the subsequent position (Figure 1B, C).

Further detailed analysis of the rosettes with strongly deviated angles showed that angles of around 180 ° were frequently observed, which is typical for a distichous rather than a spiral phyllotaxis (Figure 1C, D, E). Considering the variation in phenotypes, we

classified the observed divergence angles in 5 groups: 1) 135 ± 25 ° typical for a spiral phyllotaxis, 2) 90 ±20 ° typical for a two opposite leaves per node decussate phyllotaxis and 3) 180 ±20 ° typical for a distichous phyllotaxis, and 4) smaller than 70 ° than or 5) larger than 200 °, typical for respectively additional- or lack of primordium initiation. Interestingly, angles of 70 ° or smaller were only observed in *wag1 wag2* or *pid wag1* mutant rosettes, whereas angles larger than 200 ° were observed significantly more in *pid wag2* mutant rosettes, and a few times in *pin1 PIN1::PIN1:GFP S123A*. In *pid wag1 wag2* triple mutant rosettes a 270 ° angle was observed only once, confirming the antagonistic action between WAG1 and WAG2, and that their dual activity is needed for correct spacing of organ initiation during spiral phyllotaxis. We found that *35S::PID*, *pin1 PIN1::PIN1:GFP S123E* and *wag1 wag2* rosettes showed significantly more 90 ±20 ° angles compared to wild type (Figure 2). In *pid wag1*, *pid wag2*, *pid wag1 wag2* and *pin1 PIN1::PIN1:GFP S123A* rosettes both 90 ±20 ° and 180 ±20 ° angles were significantly increased. The results indicate that proper regulation of PIN1 phosphorylation by the AGC3 kinases is important for maintaining the spiral phyllotaxis, and that loss-of-phosphorylation, and in a milder version also enhanced phosphorylation results in a switch from spiral to a decussate-like phyllotaxis.

TCH3 regulates inflorescence phyllotaxis

Several recent publications have reported on the involvement of mechanical stress in the SAM or IM as an important determinant of phyllotaxis (Dumais and Steele, 2000; Hamant et al., 2008; Uyttewaal et al., 2012). One way mechanical stress links to PAT is by reorientation of the microtubule cytoskeleton, which was found to show co-alignment with the polar distribution of PIN1, suggesting a role for the microtubules in directing PIN1 polarity (Heisler et al., 2010). Another way mechanical stress could link to the direction of PAT is by regulating the activity of the AGC3 kinases. An interesting candidate for this regulation is the CML TCH3, as *TCH3* was initially identified as a mechanical stress-induced gene (Braam and Davis, 1990), and we previously found that TCH3 negatively regulates PID and WAG2 activity by sequestering these protein kinases from the PM, thereby affecting PIN polarity (Chapter 2).

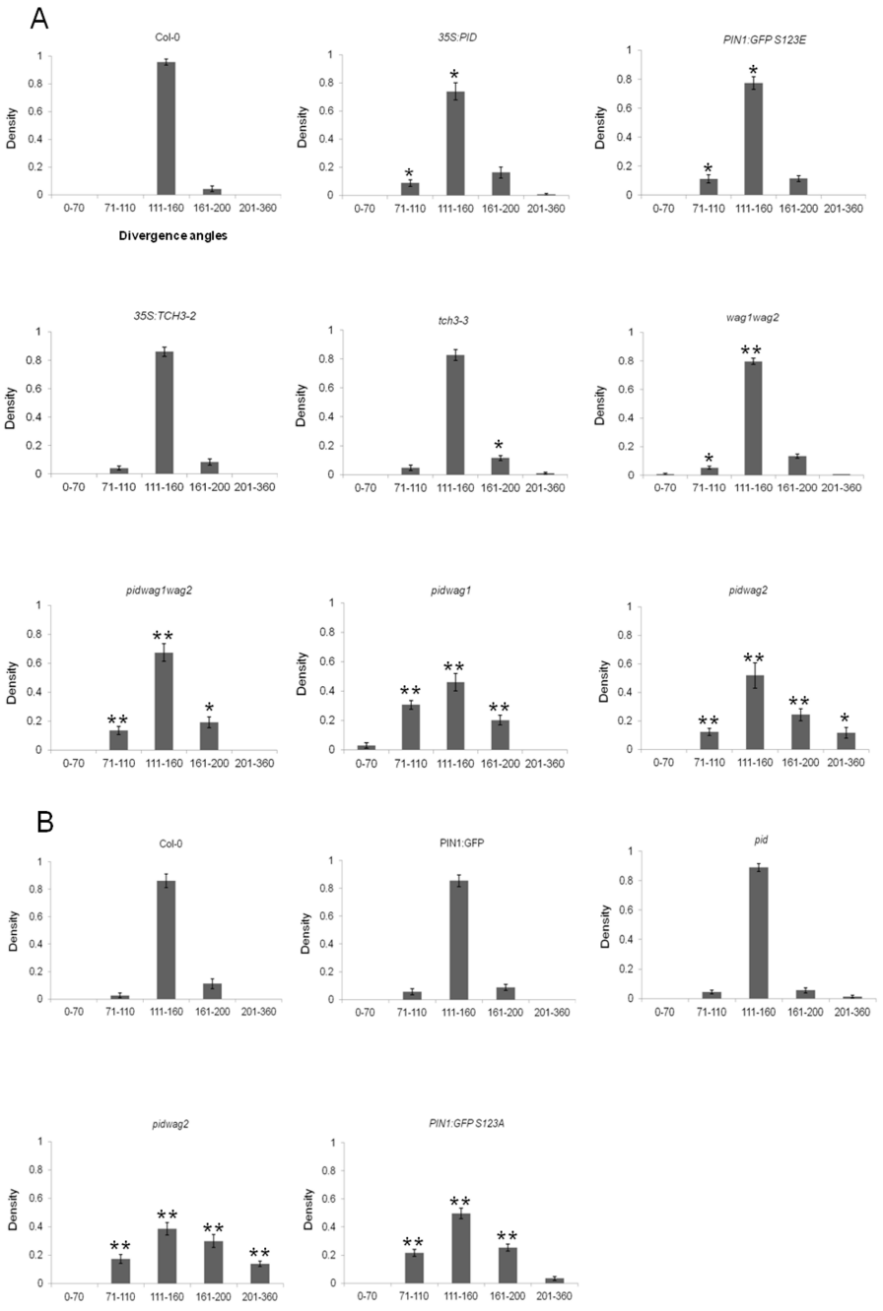

Figure 2. Divergence angle distribution in rosettes of (**A**, **B**) wild-type *Arabidopsis* (Col-0) or of the indicated

mutant plants

A and B represent two independent experiments. Asterisks indicate group values that are significantly different between mutant and Col-0 rosettes: *p<0.05; **p<0.01 (Student's *t*-test).

Both *tch3-3* loss-of-function mutant and *35S::TCH3-2* overexpression rosettes showed mild differences compared to wild-type. For *tch3-3* rosettes significantly more divergence angles around 180 ° were observed, whereas for *35S::TCH3-2* plants, the variation in the divergence angle was significantly higher compared to wild-type (Table 1, Figure 2A). In inflorescences, however, both *tch3-3* loss-of-function and *35S::TCH3-2* overexpression resulted in a significant increase in the variation of the divergence angle (Table 2), suggesting that TCH3 might be more actively involved in controlling inflorescence phyllotaxis, or that other redundantly acting CaMs of CML proteins act more predominantly in the SAM (Chapter 3). Earlier studies reported the expression of *TCH3* in the SAM (Antosiewicz et al., 1995; McCormack et al., 2005). However, in our hands the *TCH3pro::TCH3-GUS* (Sistrunk et al., 1994) or *TCH3pro::TCH3-mRFP* (Chapter 2) reporter lines only showed a very weak signal in either the SAM or IM, so the exact location of *TCH3* expression in these tissues remains to be investigated (results not shown).

As phyllotaxis is determined by PIN-driven auxin maxima that initiate lateral organ formation, we investigated the quality of the *DR5::GFP*-reported auxin maxima in *TCH3* overexpression or *tch3* loss-of-function IMs. In the *tch3-3* IMs, *DR5:GFP* was clearly expressed in the incipient primordia, and compared to a wild-type IM, the signal was slightly stronger (Figure 3A, C, D). In the *35S:TCH3-2* background, the *DR5::GFP* signal was much stronger than in wild-type IMs (Figure 3A, B, D). These results suggest that a balanced level of *TCH3* expression is required for proper phyllotaxis, and that possibly *TCH3* expression in the boundary regions, which are regions of mechanical stress [26], and exclusion of *TCH3* expression from the incipient primoridia is important in positioning and confining the auxin maxima, leading to regular spiral phyllotaxis.

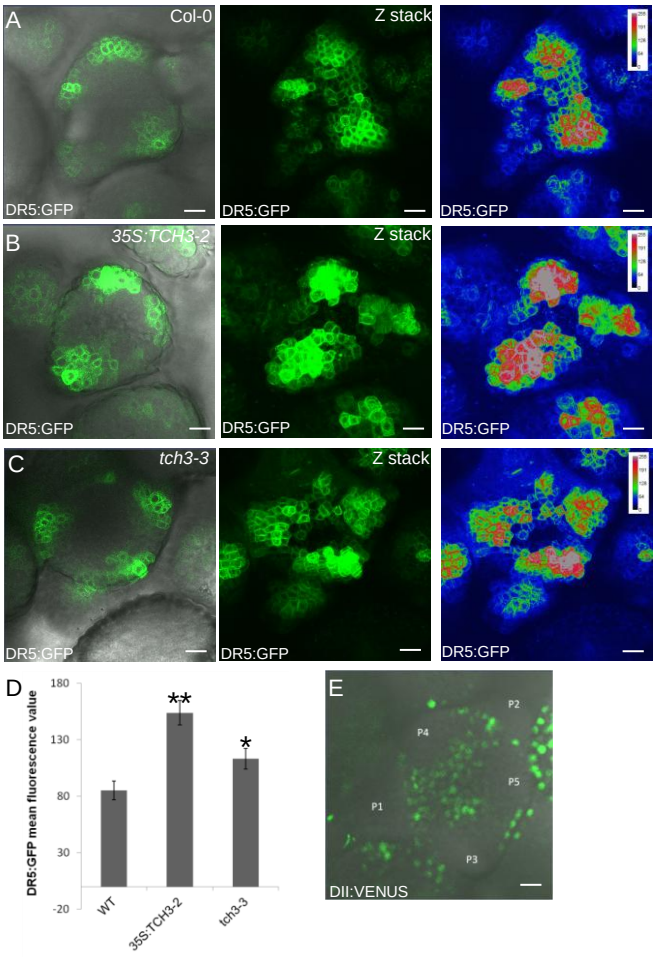

Figure 3. *TCH3* functions in inflorescence meristems (IMs). (A-C) Confocal images of the expression pattern of the *DR5::GFP* auxin response reporter in IMs of wild-type (Col-0, A), *tch3-3* (B) and *35S:TCH3-2* (C) plants. From left to right: overlay of GFP and transmitted light signal at a single focal plane, reconstructed Z-stack showing GFP signal, and reconstructed Z-stack after changing to the look up table to color-code signal intensity (low to high = blue to red). (D) Quantification of the *DR5::GFP* signal in organ primordia. *p<0.05; **p<0.01 (*t*-test). (E) Confocal image of *35S::DII-VENUS* expression in the IM. Numbered from oldest (P1) to youngest (P5) primordium. The scale bars indicate 10 μm.

Auxin and mechanical stress induce TCH3-mediated PID internalization in the inflorescence meristem

In Chapter 2 we showed that TCH3 sequesters PID from the plasma membrane (PM) to the cytoplasm in the presence of auxin, as auxin triggers elevation of $[Ca^{2+}]_{cyt}$. Mechanical stress has also been reported to cause rapid elevation of $[Ca^{2+}]_{cyt}$ (Monshausen et al., 2009), and TCH3 (and other redundant CaMs or CMLs) might play a role in translating mechanical stress into a phyllotactic pattern by internalizing PID in regions of mechanical stress, resulting in relocalization of PIN1 auxin efflux carriers.

Analysis of *PID::PID-VENUS* IMs by confocal microscopy confirmed previous observations that *PID* expression is highest in the boundaries between the meristem and the newly formed primordia (Christensen et al., 2000; Furutani et al., 2004).

In untreated meristems, PID was mainly localized at the PM, and only a few cells showed clear PID internalization (Figure 4A-C). Predominant expression of the auxin minimum reporter *35S::DII-VENUS* in the boundaries (Figure 3E), and restriction of *DR5::GFP* reporter expression to the primordia (Figure 3A) indicated that auxin levels in the boundaries are low, making it unlikely that auxin would contribute to the elevation in $[Ca^{2+}]_{cyt}$ in these regions. PID internalization was mostly observed in boundary cells between adjacent primordia, initially suggesting that these are regions of higher mechanical stress (Fig. 4B, C). However, when studying the *DR5::GFP* and *35S::DII-VENUS* images more carefully, we discovered that the boundaries between specific primordia showed a significant auxin response (Fig. 3A, E), suggesting that the observed PID internalization could be caused by both auxin and mechanical stress.

To test whether the PID internalization response to auxin observed before in *Arabidopsis* protoplasts and roots (Chapter 2) could also be observed in the IM, 5 µM NAA was applied to the meristem. Only after 2 hours treatment (and not after 5, 10, 20 or 30 minutes), PID internalization could be observed in the entire NAA treated meristem (Fig. 4E), whereas control treatments with DMSO did not result in internalization of PID (Fig. 4D). Pretreatment with the Ca^{2+} channel blocker lanthanum chloride prior to auxin application prevented PID internalization (Fig. 4F), indicating that Ca^{2+} is necessary for auxin-triggered PID internalization. In the *tch3-3* mutant background, clear PID internalization could only be observed after 4 hours of auxin application (Fig. 4H), but not after 2 hours (Fig.4G), indicating that PID internalization is delayed in this mutant background, and that like in the root tip, TCH3 is also involved in the auxin-triggered PID internalization in the IM.

In order to investigate whether mechanical stress could lead to changes in PID

subcellular localization, a cover glass was placed on the IM. This resulted in rapid internalization of PID after 30 minutes (Fig. 4I). However, when the IM was pretreated with lanthanum chloride before placing the cover glass, PID remained at the plasma membrane as in untreated samples (Fig. 4J). In the *tch3-3* mutant background, we did not observe a clear delay in mechanical stress-induced PID internalization (Fig. 4K). The results can be explained in two ways, one is TCH3 itself is not involved in mechanical stress-induced PID internalization in the meristem, which is in line with its low expression in these tissues (data not shown, (McCormack et al., 2005)). Alternatively, the CaMs and CMLs interacting with PID are acting redundantly in the SAM/IM, which fits with our observations in the root tip (Chapter 2).
In IMs of *TCH3* overexpression lines we observed PID internalization even without any treatment (Figure 4N), which is similar to what was observed in the root tip (Chapter 2). The lack of a strong phenotype in this line suggests that PID is not constitutively internalized, but rather that due to *TCH3* overexpression this line is hypersensitive to mechanical stimuli, and that internalization is due to manipulation of the IM during microscopy. Although the effects of *tch3-3* loss-of-function on phyllotaxis are mild, and the expression of *TCH3* in the SAM/IM is not detectable, the TCH3-induced internalization of PID and the observed effect of TCH3 overexpression on phyllotaxis, indicates that et least some CaM/CML proteins act redundantly in the SAM and IM to translate mechanical/auxin signals into phyllotactic patterns, by modulating PAT through internalization of PID.

Discussion

The regular pattern of organ formation in the SAM and IM, or phyllotaxis is in part determined by the unequal distribution of auxin in the L1 layer of the meristem, which is generated by the asymmetric subcellular distribution of PIN1 auxin efflux carriers (Reinhardt et al., 2003; Guenot et al., 2012; Kierzkowski et al., 2012). The polar localization of PIN1 in epidermis cells of these meristems is very dynamic (Heisler et al., 2005) and is directed by the phosphorylation status of its large central hydrophilic loop through the antagonistic action of PP2A/PP6 phosphatases on the one hand, and the AGC3 protein kinases PID, WAG1 and WAG2 on the other (Friml et al., 2004; Michniewicz et al., 2007; Dhonukshe et al., 2010; Huang et al., 2010). Moreover, PIN1 polar localization has been shown to correlate with the direction of mechanical stress (Heisler et al., 2010) and to respond to osmo-mechanical stress treatments (Nakayama et

al., 2012). In Chapters 2 and 3 we showed that the activity of the AGC3 kinases PID and WAG2 is regulated by sequestration of these kinases from the PM to the cytosol by the Ca^{2+}-dependent interaction with the CML TCH3 and closely related CaMs/CMLs. Since mechanical stress is known to induce *TCH3* expression (Braam and Davis, 1990), and at the same time leads to a rapid increase in the $[Ca^{2+}]_{cyt}$ (Monshausen et al., 2009), the AGC3 kinase–CML/CaM signaling complex is a candidate module that might be involved in translating mechanical signals into changes in PIN polarity during phyllotaxis.

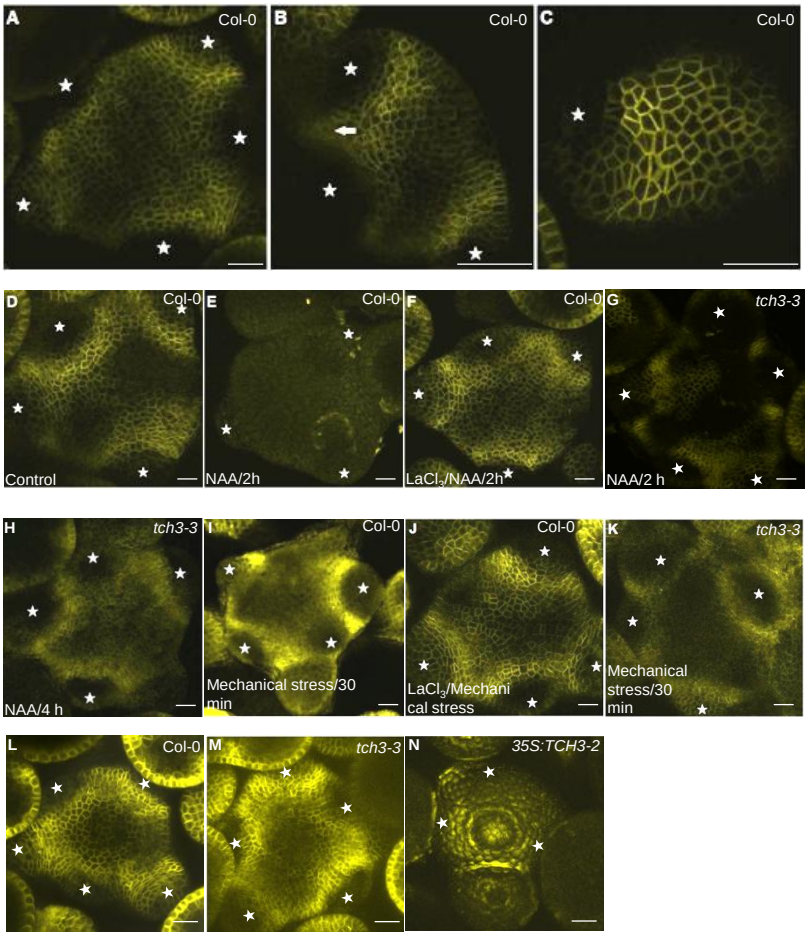

Figure 4. Ca^{2+}-dependent internalization of PID:VENUS in IMs following auxin and mechanical stress treatment. (**A-C**) PID is mostly plasma membrane localized in untreated wild-type *Arabidopsis* (Col-0) IMs.

Between primordia, PID is internalized (**B**, arrow). (**D-K**) Subcellular localization of PID-VENUS in wild–type (Col-0) (D-F,I,J,L), *tch3*-3 (G,H,K) IMs following 2 hours control treatment (D), 2 hours treatment with 5 μM NAA (E,G), 4 hours treatment with 5 μM NAA (H), 30 minutes pretreatment with 1.25 mM of the Ca^{2+} channel blocker $LaCL_3$ followed by 2 hours treatment with 5 μM NAA (F),30 minutes mechanical stress (covering with a cover glass, I,K), or pretreatment with 1.25 mM $LaCL_3$ followed by 30 minutes mechanical stress (**J**). (**L-N**) PID-VENUS is predominantly at the plasmamembrane in wild-type (Col-0, **L**) or *tch3-3* (**M**) IMs, but is mostly internalized in the *35S:TCH3-2* overexpression background (N). Primoridium tips are marked with asterisks. The scale bar indicates 10 μm.

Here we studied the possible involvement of the AGC3 kinases and the CML TCH3 in phyllotaxis. Our results show that the AGC3 kinases PID, WAG1 and WAG2 are redundantly involved in maintaining the normal spiral phyllotaxis in *Arabidopsis*, and that deregulation of PIN1 phosphorylation dynamics leads to irregularities, such as defective initiation, resulting in a 270 ° divergence angle, and in switches from the spiral (137.5 °) to a decussate-like (90/180 °) phyllotaxis. These defects were most apparent in the *pid wag2* loss-of-function mutant and in *pin1* mutant plants expressing the PIN1-GFP S>A loss-of-phosphorylation version. A defective primordium initiation can be explained by the inability to sufficiently focus PIN1-driven auxin transport in order to accumulate auxin at the next position in the L1 layer of the meristem. Based on the mutant studies, this seems to specifically require PIN1 phosphorylation by PID and WAG2.

Remarkably, in the *pid wag1 wag2* triple mutant these major phyllotaxis defects seemed to be restored, which points to the opposite effect of the *wag1* and the *wag2* mutation on the divergence angle, and suggests that, besides their redundant function in controlling spiral phyllotaxis, WAG1 and WAG2 also act antagonistically. On the one hand, their opposite effect might relate to a difference in their tissue-specific expression, and on the other it may relate to the fact that WAG2 activity is sensitive to auxin and mechanical stress through its interaction with CaM/CMLs, whereas WAG1 is not (Chapter 3).

The exact role of the CML TCH3 in the rosette phyllotaxis is not clear, as *tch3-3* loss-of-function only had mild effects on phyllotaxis, but changes in its activity led to enhanced variation in the divergence angle between primordia in the IM. Our results suggest the involvement of the AGC3 kinase-calmodulin signalling complex in controlling the phyllotactic pattern, in response to auxin and mechanical stress dynamics in the *Arabidopsis* SAM and IMs.

The switch from spiral to decussate-like phyllotaxis that we observed in the *pid wag2*

double mutant and in the *PIN1-GFP S>A* line was previously also reported for the first few rosette leaves of *pin1* mutant plants, for plants grown on the PAT inhibitor NPA and for plants mutated in *PLETHORA* genes (Prasad et al., 2011). For the *pin1* mutant plants it was suggested that this aberrant pattern was induced by the absence of one of the cotyledons (Guenot et al., 2012). In fact, in the *pid wag1 wag2* triple mutant seedlings, which lack cotyledons, we observed that the first two sets of true leaves showed a distichous phyllotaxis that is normally observed for the cotyledons and first true leaves in wild-type seedlings. This suggests that the process of cotyledon initiation during *Arabidopsis* embryogenesis is important for the subsequent onset of the spiral phyllotaxis. Apparently, the first true leaves initiated in *pid wag1 wag2* triple mutant can replace the cotyledons, so that the phyllotaxis of subsequent leaves is relatively normal, except for the larger variation in the divergence angle, which was observed for most of the mutant plants analysed (Table 1). The shift from spiral to decussate-like phyllotaxis might be explained by a higher or lower auxin amount pointing the location of the new primordium, resulting in a higher or lower inhibitory field around the primordium, and causing the new primordium to be formed respectively closer (90 °) or further away (180 °) from the last primordium.

To further investigate the involvement of mechanical stress in regulation of phyllotaxis by influencing polar auxin transport, the PID subcellular localization in IMs was studied. It has been previously shown that external auxin application leads to rapid TCH3-mediated PID internalization in a Ca^{2+}-dependent manner in protoplasts and roots (Chapter 2). The present study showed that external application of auxin or mechanical stress also leads to PID internalization in IMs. Mechanical stress, as well as auxin, can lead to an increase in the $[Ca^{2+}]_{cyt}$ within seconds (Trewavas and Knight, 1994; Haley et al., 1995). However, much more time was needed for PID internalization to occur; PID internalization in meristems was only visible after two hours treatment with auxin, while in roots internalization was observed within five minutes of auxin treatment. Despite this difference in time requirement, the finding that PID is not internalized in control meristems and in lanthanum pretreated meristems indicates that the observed internalization is caused by auxin-mediated Ca^{2+} signaling. The 2 hour time frame needed might relate to the general insensitivity of the IM to auxin or stress treatment. At the same time, in view of our problems to detect *TCH3* expression in the SAM or IM, the amount of TCH3 protein present in IM cells might be insufficient for efficient PID internalization, and an auxin- or mechanical stress-induced increase in *TCH3* expression levels (Antosiewicz et al., 1995) might be needed.

If intrinsic mechanical stress influences PIN1 localization via TCH3, it is expected that PID would be internalized in regions of the meristem experiencing high levels of mechanical stress. In the present study it was shown that PID is internalized between neighboring primordia, where mechanical stress might indeed be high due to the turgor pressure. Models predict mechanical stress to be high in the boundary between the primordia and the meristem (Hamant et al., 2008), and a switch in PIN1 polarity has been predicted there (Heisler et al., 2005), which could be caused by a change in PID activity and localization. However, at this position PID was found to be localized mainly at the plasma membrane of boundary cells, as in the centre of the meristem, where the auxin minimum localized. These data suggest that PID is not internalized as a result of intrinsic mechanical stress in this region.

Beside intrinsic mechanical stress, the meristem can experience external mechanical stress. The present study indicates that external application of mechanical stress leads to PID internalization. The prevention of mechanical stress induced PID internalization by treatment with a Ca^{2+} channel blocker implies that Ca^{2+} is involved in the signaling pathway. Since 30 minutes stress treatment was sufficient to inducePID internalization, and *TCH3* transcription is known to be upregulated by mechanical stress within this time span by touch stimulation (Braam and Davis, 1990) and increased $[Ca^{2+}]_{cyt}$ (Braam, 1992), the observed PID internalization could be caused by TCH3. In the *35S:TCH3-2* line, PID-VENUS was strongly internalized, suggesting that TCH3 and/or redundantly acting CaM/CMLs (Chapter 3) could be involved in the mechanical stress-regulated phyllotaxis.

Our analysis has shown that some CaMs and CMLs can interact with PID and lead to PID internalization (Chapter 3). Possibly, one or more of these proteins is involved in the observed PID internalization in the IM in response to auxin or touch. It has been reported that *CAM1-7* and several *CML* genes are strongly expressed in the inflorescence (McCormack et al., 2005). Moreover, besides *TCH3*, 11 other genes encoding CAM/CMLs were shown to be upregulated by touch (Lee et al., 2005), indicating that these proteins are important for the plant's response to mechanical stress. Based on the results presented in Chapter 3, especially the touch-inducible *CAM2/TCH1* and *CML10* genes are of interest here. It would be interesting to investigate if plants mutated in these *CAM/CML* genes show irregularities in phyllotaxis and to study the expression of these genes in undisturbed and touch stimulated meristems.

Finally, it is well established now that PID, WAG1 and WAG2 act redundantly in directing PIN polar localization (Dhonukshe et al., 2010), but the phenotypic analysis

presented here indicates that WAG1 and WAG2 act antagonistically in the establishment of the phyllotactic pattern. For a deeper insight into the antagonistic behavior of these kinases it will be necessary to study their expression and subcellular localization in the meristem in more detail.

Experimental Procedures

Arabidopsis lines and plant growth

The *Arabidopsis thaliana* (col-0) *35S::PID-21*, *DR5rev::GFP*, *35S::DII-VENUS*, *TCH3::TCH3-GUS*, *PID::PID-VENUS*, *PIN::PIN1-GFP*, *PIN1::PIN1-GFP S123A* and *PIN1::PIN1-GFP S123E* lines and *pid-14*, *wag1* and *wag2* single, double and triple mutants have been described previously (Sistrunk et al., 1994; Benjamins et al., 2001; Benkova et al., 2003; Michniewicz et al., 2007; Dhonukshe et al., 2010; Huang et al., 2010; Brunoud et al., 2012). The *TCH3::TCH3-mRFP* and *35S::TCH3-2* lines and the *tch3-3* mutant, have been described in Chapter 2.

Arabidopsis seeds were surface sterilized by washing in 70% ethanol, incubating for 8 minutes in 50% commercial bleach, and washing six times with sterile water. Seeds were stored at 4 ℃ for two to three days and germinated on solid MA medium (Masson and Paszkowski, 1992) at 21 ℃ and 16 hours photoperiod. Plants were transferred to soil 10-14 days after germination and grown at 21 ℃, 70% relative humidity and 16 hours photoperiod.

Phenotypic analysis

For the phenotypic analysis of Col-0, *tch3-3*, *35S::TCH3*, *35S::PID-21*, *pid-14 wag1*, *pid-14 wag2*, *pid-14 wag1 wag2*, *wag1 wag2* and *PIN::PIN1-GFP S123E* plant lines, pictures of rosettes were taken when the plants were 14-, 19- and 26-day-old. The pictures of 14- and 19-day-old plants were used to determine the order of initiation of rosette leaves in the 26-day-old plants. Angles between subsequent leaves were measured from the pictures of 26-day-old plants. Angles between subsequent pedicels in inflorescences were determined from pictures of inflorescences of six to eight week old plants. For the phenotypic analysis of Col-0, *pid-14*, *pid-14 wag2*, *PIN1:GFP* and *PIN1:GFP S123A* plant lines, pictures of rosettes were taken when plants were 19- and 27-days-old and pictures of 27-day-old plants were used to measure divergence angles. Divergence angles in primary inflorescences of Col-0 and *PIN1:GFP* plants were measured from pictures of inflorescences of 5-week-old plants and divergence angles of

secondary inflorescences were determined using pictures of inflorescences of 6-week-old plants.

Statistical analysis

The F-test was used for comparing variances between plant lines and the Pearson's Chi squared test was used for comparing the number of divergence angles bigger than 180 º per line. The Student's *t*-test was used to compare the divergence angle distribution and *DR5::GFP* fluorescence intensities between mutant lines and wild-type *Arabidopsis*.

Histochemical staining and microscopy

Seedlings were stained for GUS activity as described (Benjamins et al., 2001) and analyzed using a Zeiss Axioplan II microscope with DIC optics. Images were recorded with a ZEISS AxioCam MRc5 camera. IMs of *PID::PID-VENUS* and *tch3-3/PID::PID-VENUS* plants were dissected and put in a drop of 1% low melting point agarose. Chemical and mechanical treatments were performed after dissection. To apply mechanical stress a cover glass was put on the meristem and the sample was observed after removal of the cover glass or with the cover glass remaining on the meristem. As a control, meristems were left untreated after dissection before observation. Auxin or control treatments were performed by putting a drop of liquid MA medium containing 5 µM NAA (dissolved in DMSO) or DMSO only on the meristem. When indicated, meristems were pretreated with 1.25 mM lanthanum chloride (125 mM stock in H_2O; Sigma) for 30-40 minutes before mechanical or auxin treatment. Samples were observed with a ZEISS LSM5 confocal microscope using a 40x long working distance water dipping objective or a 20x objective. PID-VENUS fluorescence was visualized with an argon laser for excitation at 514 nm and a 530-600 nm band pass emission filter. DII-VENUS fluorescence was monitored with an argon laser for excitation at 514 nm and a 530-600 nm band pass emission filter. *DR5::GFP* fluorescence was monitored using an argon laser for excitation at 488 nm and a 505-530 nm band pass emission filter. TCH3-mRFP fluorescence was monitored using an argon laser for excitation at 543 nm excitation and a 560nm long pass emission filter. Images were processed using Image J and assembled in Adobe Photoshop (http://rsb.info.nih.gov/ij/).

Acknowledgements

The authors would like to thank J.Braam for sharing her unpublished data on the *tch3-3*

allele, Teva Vernoux for sharing *35S::DII-VENUS*, Gerda Lamers, Ward de Winter and Jan Vink for their help with the microscopy, tissue culture and plant caretaking, respectively.

References

Antosiewicz, D.M., Polisensky, D.H., and Braam, J. (1995). Cellular localization of the Ca^{2+} binding TCH3 protein of *Arabidopsis*. Plant J **8,** 623-636.

Benjamins, R., Ampudia, C.S., Hooykaas, P.J., and Offringa, R. (2003). PINOID-mediated signaling involves calcium-binding proteins. Plant Physiol **132,** 1623-1630.

Benjamins, R., Quint, A., Weijers, D., Hooykaas, P., and Offringa, R. (2001). The PINOID protein kinase regulates organ development in *Arabidopsis* by enhancing polar auxin transport. Development **128,** 4057-4067.

Benkova, E., Michniewicz, M., Sauer, M., Teichmann, T., Seifertova, D., Jurgens, G., and Friml, J. (2003). Local, efflux-dependent auxin gradients as a common module for plant organ formation. Cell **115,** 591-602.

Besnard, F., Vernoux, T., and Hamant, O. (2011). Organogenesis from stem cells in planta: multiple feedback loops integrating molecular and mechanical signals. Cell Mol Life Sci **68,** 2885-2906.

Braam, J. (1992). Regulated expression of the calmodulin-related *TCH* genes in cultured *Arabidopsis* cells: induction by calcium and heat shock. Proc Natl Acad Sci U S A **89,** 3213-3216.

Braam, J., and Davis, R.W. (1990). Rain-, wind-, and touch-induced expression of calmodulin and calmodulin-related genes in Arabidopsis. Cell **60,** 357-364.

Brunoud, G., Wells, D.M., Oliva, M., Larrieu, A., Mirabet, V., Burrow, A.H., Beeckman, T., Kepinski, S., Traas, J., Bennett, M.J., and Vernoux, T. (2012). A novel sensor to map auxin response and distribution at high spatio-temporal resolution. Nature **482,** 103-106.

Christensen, S.K., Dagenais, N., Chory, J., and Weigel, D. (2000). Regulation of auxin response by the protein kinase PINOID. Cell **100,** 469-478.

Dhonukshe, P., Huang, F., Galvan-Ampudia, C.S., Mahonen, A.P., Kleine-Vehn, J., Xu, J., Quint, A., Prasad, K., Friml, J., Scheres, B., and Offringa, R. (2010). Plasma membrane-bound AGC3 kinases phosphorylate PIN auxin carriers at TPRXS(N/S) motifs to direct apical PIN recycling. Development **137,** 3245-3255.

Dumais, J., and Steele, C.R. (2000). New evidence for the role of mechanical forces in the shoot apical meristem. J Plant Growth Regul **19,** 7-18.

Friml, J., Yang, X., Michniewicz, M., Weijers, D., Quint, A., Tietz, O., Benjamins, R., Ouwerkerk, P.B., Ljung, K., Sandberg, G., Hooykaas, P.J., Palme, K., and Offringa, R. (2004). A PINOID-dependent binary switch in apical-basal PIN polar targeting directs auxin efflux. Science **306,** 862-865.

Furutani, M., Vernoux, T., Traas, J., Kato, T., Tasaka, M., and Aida, M. (2004). *PIN-FORMED1* and *PINOID* regulate boundary formation and cotyledon development in *Arabidopsis* embryogenesis. Development **131,** 5021-5030.

Guenot, B., Bayer, E., Kierzkowski, D., Smith, R.S., Mandel, T., Zadnikova, P., Benkova, E., and Kuhlemeier, C. (2012). Pin1-independent leaf initiation in Arabidopsis. Plant Physiol **159,** 1501-1510.

Haley, A., Russell, A.J., Wood, N., Allan, A.C., Knight, M., Campbell, A.K., and Trewavas, A.J. (1995). Effects of mechanical signaling on plant cell cytosolic calcium. Proc Natl Acad Sci U S A **92,** 4124-4128.

Hamant, O., Heisler, M.G., Jonsson, H., Krupinski, P., Uyttewaal, M., Bokov, P., Corson, F., Sahlin, P., Boudaoud, A., Meyerowitz, E.M., Couder, Y., and Traas, J. (2008). Developmental patterning by mechanical signals in *Arabidopsis*. Science **322,** 1650-1655.

Heisler, M.G., Ohno, C., Das, P., Sieber, P., Reddy, G.V., Long, J.A., and Meyerowitz, E.M. (2005). Patterns of auxin transport and gene expression during primordium development revealed by live imaging of the *Arabidopsis* inflorescence meristem. Curr Biol **15,** 1899-1911.

Heisler, M.G., Hamant, O., Krupinski, P., Uyttewaal, M., Ohno, C., Jonsson, H., Traas, J., and Meyerowitz, E.M. (2010). Alignment between PIN1 polarity and microtubule orientation in the shoot apical meristem reveals a tight coupling between morphogenesis and auxin transport. PLoS Biol **8,** e1000516.

Huang, F., Zago, M.K., Abas, L., van Marion, A., Galvan-Ampudia, C.S., and Offringa, R. (2010). Phosphorylation of conserved PIN motifs directs *Arabidopsis* PIN1 polarity and auxin transport. Plant Cell **22,** 1129-1142.

Jonsson, H., Heisler, M.G., Shapiro, B.E., Meyerowitz, E.M., and Mjolsness, E. (2006). An auxin-driven polarized transport model for phyllotaxis. Proc Natl Acad Sci U S A **103,** 1633-1638.

Kierzkowski, D., Nakayama, N., Routier-Kierzkowska, A.L., Weber, A., Bayer, E.,

Schorderet, M., Reinhardt, D., Kuhlemeier, C., and Smith, R.S. (2012). Elastic domains regulate growth and organogenesis in the plant shoot apical meristem. Science **335,** 1096-1099.

Kuhlemeier, C. (2007). Phyllotaxis. Trends Plant Sci **12,** 143-150.

Landrein, B., Lathe, R., Bringmann, M., Vouillot, C., Ivakov, A., Boudaoud, A., Persson, S., and Hamant, O. (2013). Impaired cellulose synthase guidance leads to stem torsion and twists phyllotactic patterns in *Arabidopsis*. Curr Biol **23,** 895-900.

Lee, D., Polisensky, D.H., and Braam, J. (2005). Genome-wide identification of touch- and darkness-regulated Arabidopsis genes: a focus on calmodulin-like and *XTH* genes. New Phytol. **165,** 429-444.

McCormack, E., Tsai, Y.C., and Braam, J. (2005). Handling calcium signaling: *Arabidopsis* CaMs and CMLs. Trends Plant Sci **10,** 383-389.

Michniewicz, M., Zago, M.K., Abas, L., Weijers, D., Schweighofer, A., Meskiene, I., Heisler, M.G., Ohno, C., Zhang, J., Huang, F., Schwab, R., Weigel, D., Meyerowitz, E.M., Luschnig, C., Offringa, R., and Friml, J. (2007). Antagonistic regulation of PIN phosphorylation by PP2A and PINOID directs auxin flux. Cell **130,** 1044-1056.

Mirabet, V., Das, P., Boudaoud, A., and Hamant, O. (2011). The role of mechanical forces in plant morphogenesis. Annu Rev Plant Biol **62,** 365-385.

Mitchison, G.J. (1977). Phyllotaxis and the fibonacci series. Science **196,** 270-275.

Monshausen, G.B., Bibikova, T.N., Weisenseel, M.H., and Gilroy, S. (2009). Ca^{2+} regulates reactive oxygen species production and pH during mechanosensing in *Arabidopsis* roots. Plant Cell **21,** 2341-2356.

Nakayama, N., Smith, R.S., Mandel, T., Robinson, S., Kimura, S., Boudaoud, A., and Kuhlemeier, C. (2012). Mechanical regulation of auxin-mediated growth. Curr Biol **22,** 1468-1476.

Newell, A.C., Shipman, P.D., and Sun, Z. (2008). Phyllotaxis: cooperation and competition between mechanical and biochemical processes. J Theor Biol **251,** 421-439.

Prasad, K., Grigg, S.P., Barkoulas, M., Yadav, R.K., Sanchez-Perez, G.F., Pinon, V., Blilou, I., Hofhuis, H., Dhonukshe, P., Galinha, C., Mahonen, A.P., Muller, W.H., Raman, S., Verkleij, A.J., Snel, B., Reddy, G.V., Tsiantis, M., and Scheres, B. (2011). *Arabidopsis* PLETHORA transcription factors control phyllotaxis. Curr Biol **21,** 1123-1128.

Reinhardt, D., Frenz, M., Mandel, T., and Kuhlemeier, C. (2005). Microsurgical and laser ablation analysis of leaf positioning and dorsoventral patterning in tomato.

Development **132,** 15-26.

Reinhardt, D., Pesce, E.R., Stieger, P., Mandel, T., Baltensperger, K., Bennett, M., Traas, J., Friml, J., and Kuhlemeier, C. (2003). Regulation of phyllotaxis by polar auxin transport. Nature **426,** 255-260.

Sistrunk, M.L., Antosiewicz, D.M., Purugganan, M.M., and Braam, J. (1994). Arabidopsis *TCH3* encodes a novel Ca^{2+} binding protein and shows environmentally induced and tissue-specific regulation. Plant Cell **6,** 1553-1565.

Smith, R.S., Guyomarc'h, S., Mandel, T., Reinhardt, D., Kuhlemeier, C., and Prusinkiewicz, P. (2006). A plausible model of phyllotaxis. Proc Natl Acad Sci U S A **103,** 1301-1306.

Tanaka, H., Dhonukshe, P., Brewer, P.B., and Friml, J. (2006). Spatiotemporal asymmetric auxin distribution: a means to coordinate plant development. Cell Mol Life Sci **63,** 2738-2754.

Trewavas, A., and Knight, M. (1994). Mechanical signalling, calcium and plant form. Plant Mol Biol **26,** 1329-1341.

Uyttewaal, M., Burian, A., Alim, K., Landrein, B., Borowska-Wykret, D., Dedieu, A., Peaucelle, A., Ludynia, M., Traas, J., Boudaoud, A., Kwiatkowska, D., and Hamant, O. (2012). Mechanical stress acts via katanin to amplify differences in growth rate between adjacent cells in *Arabidopsis*. Cell **149,** 439-451.